PNAS RESEARCH ARTICLE | ECOLOGY

Evidence for adaptive morphological plasticity in the Caribbean coral, *Acropora cervicornis*

Wyatt C. Million[a,1], Maria Ruggeri[a], Sibelle O'Donnell[a], Erich Bartels[b], Trinity Conn[c], Cory J. Krediet[d], and Carly D. Kenkel[a]

Edited by Stephen Palumbi, Stanford University, Department of Biological Sciences, Pacific Grove, CA; received March 7, 2022; accepted September 15, 2022

Genotype-by-environment interactions (GxE) indicate that variation in organismal traits cannot be explained by fixed effects of genetics or site-specific plastic responses alone. For tropical coral reefs experiencing dramatic environmental change, identifying the contributions of genotype, environment, and GxE on coral performance will be vital for both predicting persistence and developing restoration strategies. We quantified the impacts of G, E, and GxE on the morphology and survival of the endangered coral, *Acropora cervicornis*, through an in situ transplant experiment exposing common garden (nursery)-raised clones of ten genotypes to nine reef sites in the Florida Keys. By fate-tracking outplants over one year with colony-level 3D photogrammetry, we uncovered significant GxE on coral size, shape, and survivorship, indicating that no universal winner exists in terms of colony performance. Rather than differences in mean trait values, we found that individual-level morphological plasticity is adaptive in that the most plastic individuals also exhibited the fastest growth and highest survival. This indicates that adaptive morphological plasticity may continue to evolve, influencing the success of *A. cervicornis* and resulting reef communities in a changing climate. As focal reefs are active restoration sites, the knowledge that variation in phenotype is an important predictor of performance can be directly applied to restoration planning. Taken together, these results establish *A. cervicornis* as a system for studying the ecoevolutionary dynamics of phenotypic plasticity that also can inform genetic- and environment-based strategies for coral restoration.

GxE | fragmentation | growth | survival | 3D photogrammetry

Intraspecific variation in phenotype provides raw material for selection to act on, resulting in the evolution of trait means (1). However, trait values may also change as individuals are exposed to different environments via phenotypic plasticity (2). While plastic trait changes typically occur within a generation, they have the ability to alter fitness-related traits and promote acclimatization and are therefore relevant for populations experiencing new or stressful environmental conditions (3–6). Moreover, variation in the degree of plasticity can magnify differences among individuals. In the light of intraspecific variation in plasticity, the evolution of trait means becomes dependent not only on individual trait values but also on the environments those individuals face. Long-standing theory supports a role for plasticity in trait evolution (7–9), and the presence of significant intraspecific variation in plasticity, i.e., genotype-by-environment interactions (GxE), suggests that plasticity itself can also evolve (10–12).

The evolution of phenotypic plasticity, and consequently its ecological impacts, can occur if variation in plasticity among individuals results in variation in fitness. Selection is expected to increase plasticity when the benefits of producing an environment-specific phenotype outweigh the fitness consequences arising from either the cost of altering that phenotype, or from the production of an imperfect phenotype relative to locally adapted individuals (13, 14). Evolutionary models suggest plasticity will be favored in species with high dispersal that will experience predictably high spatial or temporal environmental variation and when the costs of plasticity are low (14). However, limited empirical tests for an adaptive role of plasticity (12, 14) provide inconsistent support for model predictions with variation evident among traits, species, and environments (14–16). More experiments that quantify the fitness costs or benefits of plasticity, especially in nonmodel systems, will improve our broad understanding of its ecological and evolutionary role (2, 10); for example, if organismal plasticity influences community- and ecosystem-level processes (14), while also uncovering system-specific functions contributing to acclimatization to environmental change. This will be particularly important for species of conservation concern, whose persistence may be reliant on both adaptive plasticity and the ability of human interventions to leverage it.

Significance

Phenotypic plasticity, or the ability of organisms to alter traits in response to environmental change, can facilitate acclimatization, expose or buffer genetic variation, and may even evolve. Understanding how variation in plasticity among individuals impacts fitness will be critical for determining its adaptive potential during climate change, particularly for organisms incapable of behavioral escape from environmental extremes. Here, we show that morphologically plastic *Acropora cervicornis* had higher survival and growth rates than less plastic individuals. Therefore, plasticity is not only variable among *A. cervicornis*, but selection will be expected to favor its evolution. Considering the absence of a universal top grower or survivor, our results suggest environmental responsiveness will be more useful for predicting coral performance across reefs.

Author contributions: C.J.K. and C.D.K. designed research; W.C.M., M.R., S.O., E.B., C.J.K., and C.D.K. performed research; W.C.M., S.O., T.C., and C.D.K. contributed new reagents/analytic tools; W.C.M., T.C., and C.D.K. analyzed data; W.C.M., M.R., S.O., E.B., T.C., C.J.K., and C.D.K. contributed to manuscript revisions; and W.C.M. and C.D.K. wrote the paper.

The authors declare no competing interest.

This article is a PNAS Direct Submission.

Copyright © 2022 the Author(s). Published by PNAS. This article is distributed under Creative Commons Attribution-NonCommercial-NoDerivatives License 4.0 (CC BY-NC-ND).

[1]To whom correspondence may be addressed. Email: wmillion@usc.edu, ckenkel@usc.edu.

This article contains supporting information online at https://www.pnas.org/lookup/suppl/doi:10.1073/pnas.2203925119/-/DCSupplemental.

Published November 28, 2022.

Downloaded from https://www.pnas.org by NOAA CENTRAL LIBRARY on January 11, 2024 from IP address 137.75.80.24.

Reef-building corals form the base of one of the most biodiverse marine ecosystems, tropical coral reefs (17, 18). The ecological and economic services they provide are determined in part by the complex three-dimensional structures created by the corals themselves (19–21). This structure provides habitat space (22), reduces wave energy (21), and sustains biological diversity and productivity (19, 23), which support local communities in more than 100 countries and a multi-billion-dollar tourism industry (24). However, these ecosystem services are being lost as wild populations decline due to natural and anthropogenic factors (25, 26). For example, populations of *Acropora cervicornis*, one of the two branching coral species once dominating Caribbean reefs, have declined precipitously since the 1970s (27), contributing to a loss of structural complexity (28, 29). This decline has prompted a global effort to understand factors that promote coral survival and persistence under changing ocean conditions. Both differences in fitness-related traits among common-gardened genotypes and of clones under different conditions (30–33) suggest that some individuals or environments could be used to reestablish the structure and function of reefs (34–36). However, as corals experience new conditions via translocation during reef restoration (37, 38) or through climate change (39, 40), it is unclear whether top-performing genotypes will maintain their status (41, 42) or if variation in plasticity will result in new "winners" and "losers" (43). Therefore, clarifying the role of both the environment and genetic background on coral performance as well as GxE will be critical for leveraging naturally occurring biological variation for the restoration of degraded reefs.

Phenotypic plasticity has been commonly documented in coral morphology (44, 45), physiology (46, 47), and gene expression (48, 49) in response to a variety of abiotic factors, indicating the environmental responsiveness of phenotypes, some of which is correlated with fitness-related traits at the population level (50–52). Within-populations, GxE have been reported less frequently (41, 43, 53), but the relationship between phenotypic plasticity and overall fitness remains unresolved. This gap in knowledge limits both our understanding of the evolutionary potential of plasticity and its role in the natural and human-assisted recovery of coral reefs in a changing climate.

While variation in plasticity exists in wild coral populations (41, 53, 54), it is unclear whether such variation is maintained in restoration corals, like *A. cervicornis*, which may have undergone selection during decades of propagation in environmentally stable common-garden nurseries. Given that restoration involves outplanting clonal replicates (ramets) across environmentally diverse, natural reefs (37, 55), understanding how individual phenotypes vary can help direct restoration efforts. Previous efforts found no evidence of GxE in *A. cervicornis* growth despite strong site and genotype effects on linear growth and survival (33, 37, 55), but significant variation in bleaching responses among genotypes was observed across natural reefs (43). GxE in fitness-related traits, like bleaching tolerance, suggest that a multisite-based phenotype may more accurately describe *A. cervicornis* performance in nature.

We rigorously fate-tracked 270 restored coral colonies on natural reefs in a multisite transplant experiment to test the effect of genotype, environment, and their interaction on growth rate, size, risk of fragmentation, and survival (Fig. 1 *A*–*C*). We uncovered significant GxE in survival and aspects of morphology measured with 3D photogrammetry and identified relationships between morphological plasticity, growth, and survival that support the presence of adaptive plasticity in *A. cervicornis*. Taken together, our results establish a system to investigate the ecological and evolutionary impacts of adaptive plasticity while also informing reef restoration.

Results

Ramet Survival is a Function of Genotype, Outplant Site, and the Interaction. Of the 270 outplanted ramets, 48 died and 24 were declared missing, leaving 198 surviving ramets at the end of 1 y. Cox proportional hazard models showed significant effects of genotype (P = 0.005), site (P = 0.034), and fragmentation (P = 0.049), but not initial colony size (P = 0.6) on survival. The model including the interaction term, while improving fit, did not converge, so the additive model was used to obtain risk scores for each genotype and site (*SI Appendix*, Tables S2 and S3). On average, genotype (G) 36 had the highest ramet survival (96%), while G41 had the lowest (61.5%) across sites, which incurred a mortality risk 2.6 times that of G36 on average (Fig. 2*A* and *SI Appendix*, Table S2). Three genotypes (G41, G62, and G13) form a group of high-risk genets (>2.3× higher mortality risk in comparison to G36), while the remaining genets display intermediate risk ranging from nearly equivalent to 1.7 times that of G36 (Fig. 2*A* and *SI Appendix*, Table S2). Ramets outplanted to Bahia Honda (60% survival) had a 2.5 times greater risk of mortality than those outplanted to E. Sambo, the site with the highest survival on average (96.4%, Fig. 2*B*). Similar to average genotype scores, sites exhibited a continuum of increasing risk with mortality ranging from 1.1 to 2.5 times higher than the reference, E. Sambo, with the highest mortality risk occurring at Bahia Honda (*SI Appendix*, Table S3).

Pairwise correlations of genet survival ranks across sites show that the identity of the best surviving genet is not maintained across sites, with most correlations being close to 0 or nonsignificant (Fig. 2*C*). The highest positive correlations (Spearman's correlation = 0.54–0.70) were observed among sites with intermediate survival on average (Big Pine, Dave's Ledge, Looe Key, and EDR, Fig. 2*B*) and not necessarily among geographically neighboring sites (Fig. 1*A* and *SI Appendix*, Fig. S2).

Nonrandom Fragmentation in *A. cervicornis*. We documented 177 instances of fragmentation throughout this experiment. Most events occurred within the first 3 mo post-outplant (84) followed by continually decreasing occurrences in subsequent time periods. Cumulative linked models show a significant effect of genotype and site on the likelihood of fragmentation (*SI Appendix*, Table S4), with G1 and Marker 32 experiencing the least amount of fragmentation among genotypes and sites, respectively (*SI Appendix*, Fig. S3). G13 and Bahia Honda experienced the most fragmentation among genotypes and sites, respectively, during the outplant period. Of the 177 fragmentation events, only 15.8% occurred in the same time period that the ramet died, indicating that fragmentation did not result in immediate mortality. Fragmentation was not overly prevalent in larger size class colonies, and instead was more common in colonies less than 5 cm and between 5 and 10 cm in length according to Fisher's exact tests (*SI Appendix*, Table S5).

Morphology Exhibits Plasticity that Varies by Genotype (GxE). Colony morphology is tied to growth rate, patterns of calcification at gross and fine scales, and fragmentation (57). Therefore, we quantified coral morphology with a series of size-related as well as shape-related traits, the latter of which are considered more traditional descriptors (44, 58). We assessed the fixed effects of genotype, outplant site, time, their interactions, as well as initial size on the absolute size in four traits: total linear extension (TLE), surface area (SA), volume (V), and volume of interstitial space (V_{inter}) (*SI Appendix*, Table S6). Ramets experiencing fragmentation were retained, and the site-specific array to which the ramet was outplanted and the number of fragmentation events it experienced

Downloaded from https://www.pnas.org by NOAA CENTRAL LIBRARY on January 11, 2024 from IP address 137.75.80.24.

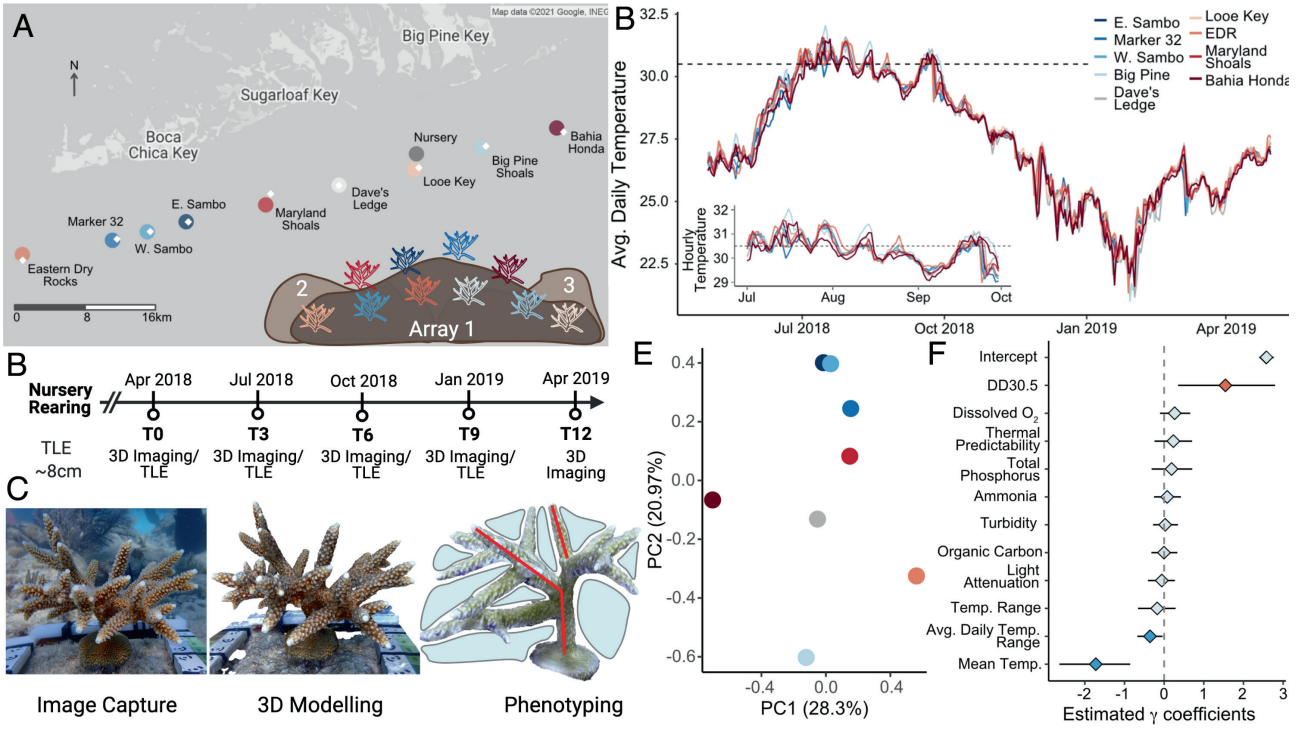

Fig. 1. Experimental design and environmental conditions (*A*) Location of outplant sites (*SI Appendix*, Table S1) and the source restoration nursery in the lower Florida Keys, USA. Ten genets (genotypes) of *A. cervicornis* sourced from the lower Florida Keys (*SI Appendix*, Fig. S1) were outplanted in triplicate to nine reef sites in three subarrays. Sites are colored by average survival from dark blue (highest) to dark red (lowest), and the location of site-specific SERC water quality monitoring stations (56) is indicated by the white diamonds. (*B*) Ramets were reared in the nursery to a mean size of 8 cm and were measured just prior to outplanting in April 2018 (*C*) To obtain growth and morphology data, still images were captured using underwater photography, which were used to build 3D models in Agisoft Metashape, that were subsequently measured for total linear extension (TLE; example red lines), surface area (SA), volume (V), and volume of the interstitial space (V_{inter}; example shaded blue area) (*D*) Average daily temperature of each site (colored by survival rank) for the 1-y experimental period. *Inset* shows hourly temperatures from July through September 2018. The dashed line indicates the local bleaching threshold of 30.5°C. (*E*) Principal component analysis of historical SERC environmental metrics characterizing outplant reef sites (Looe Key is excluded due to missing data). PCA loadings can be found in *SI Appendix*, Fig. S17. (*F*) Results of a Bayesian negative binomial generalized linear mixed effects model testing the association of eleven uncorrelated environmental parameters on the change in V_{inter}. Horizontal black lines indicate 95% credible intervals of the posterior distributions. Values above (red) or below (blue) indicate significant association between the variable and the change in V_{inter} across sites.

were included as random effects (*SI Appendix*, Table S7). Significant genotype-by-site interactions were detected in all four traits ($P < 0.001$), whereas no effects were detected for the genotype-by-time and genotype-by-site-by-time interactions in any trait ($P > 0.05$). Absolute size trajectories varied among genets and inconsistent genet rank order was evident across sites, confirming the existence of GxE (Fig. 3 and *SI Appendix*, Figs. S4–S6). Significant effects of genotype, time, and initial ramet size were also evident for all traits ($P < 0.0001$). Absolute trait size increased over time and with the initial size of a ramet (Fig. 3 and *SI Appendix*, Figs. S4–S6). Ramets of G50 were the largest on average, while G13's ramets were the smallest. The largest ramet sizes were reached at EDR, a

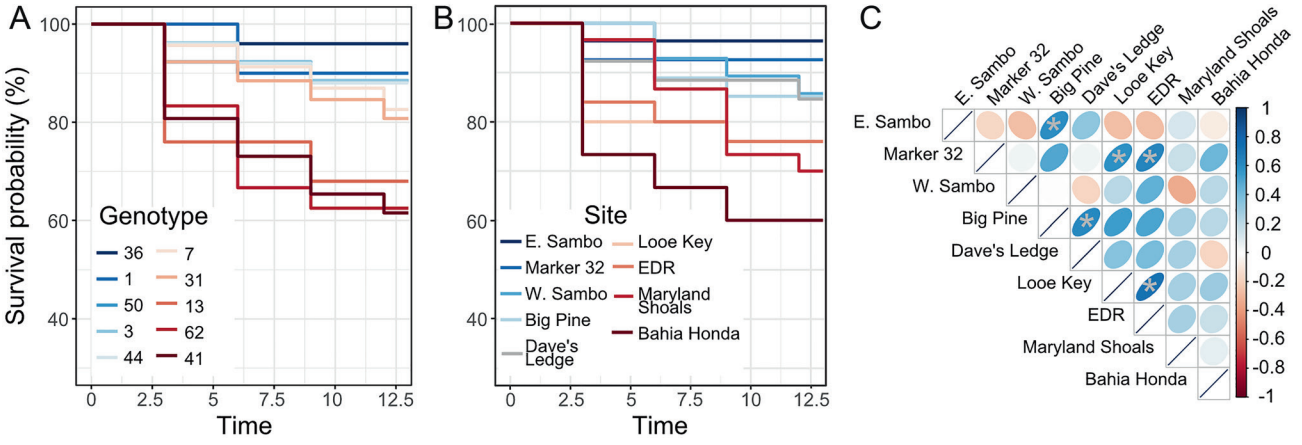

Fig. 2. Genotype, environment, and GxE patterns of survival. (*A*) Survival probability for genets and (*B*) sites over the 1-y experimental period. Genets and sites are colored by decreasing overall survival from blue to red. (*C*) Pairwise correlations of genet survival rank across outplant sites. Asterisks denote significant correlations (Spearman's correlation, $P < 0.05$). Ellipse shape and color are proportional to the strength and direction of the correlation, respectively, between two sites. Sites are ordered according to survival as in (*B*).

Downloaded from https://www.pnas.org by NOAA CENTRAL LIBRARY on January 11, 2024 from IP address 137.75.80.24.

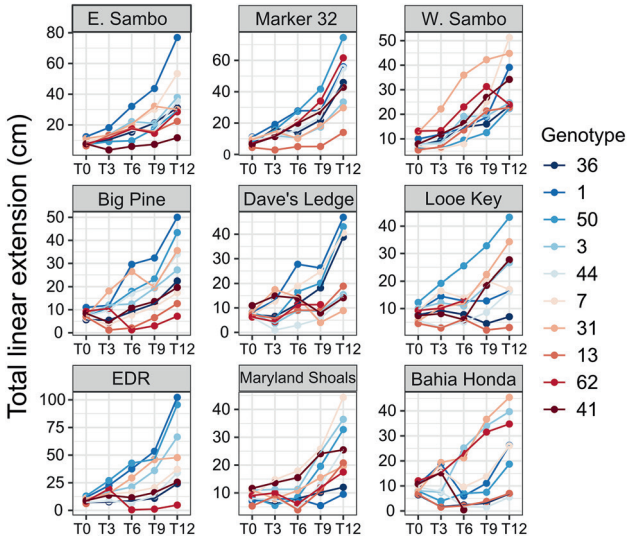

Fig. 3. Average size in total linear extension (TLE) for each genotype (colored by survival probability as in Fig. 2*A*) over time. Reef sites are also ordered by survival probability (*Left* to *Right*).

site with the third worst survival on average (Fig. 2*B*). However, significant fixed effects of outplant site were not evident, while significant site-by-time interactions were found in SA and V ($P < 0.01$). Random effects of fragmentation ($P < 0.0001$) and array within site ($P < 0.0001$) were also evident in all trait models (*SI Appendix*, Table S7).

To assess changes in colony shape independent of size, we estimated the effects of G, E, and GxE using the same linear mixed-model framework described above for five shape-related traits: SA-to-V ratio, TLE-to-V ratio, packing, convexity, and sphericity (58). Similar to the size-dependent traits, all showed significant effects of genotype and the genotype-by-site interaction ($P < 0.01$, *SI Appendix*, Table S8). Site effects were only detected for SA-to-V ($P = 0.009$) although significant site-by-time interactions were seen in four traits: SA-to-V, SA-to-TLE, sphericity, and packing ($P < 0.05$). Time had a significant effect on all traits ($P < 0.001$); however, initial shape at T0 was only significant for sphericity ($P = 0.01$). Random effects of fragmentation ($P < 0.05$) and array within site ($P < 0.05$) were also present for all five size-independent traits (*SI Appendix*, Table S9).

Growth Rate is Dependent on Genotypic and Environmental Characteristics. Growth rate (unit/month) in size-related traits (TLE, SA, V, V_{inter}) was modeled as a fixed effect of genotype, outplant site, time, and their interactions. Size at the beginning of each time interval was included as a fixed effect in linear mixed models to account for potential size-specific growth rates (*SI Appendix*, Table S10). To accurately quantify growth rate, time periods where a ramet experienced negative growth due to fragmentation were excluded from the mixed models, following (33). Fragmentation and the site-specific array to which the ramet was outplanted were included as random effects (*SI Appendix*, Table S11) and despite being removed from the analysis, a moderate effect of fragmentation persisted for V ($P = 0.11$). Genotype-by-site and the three-way interaction between genotype, site, and time were not significant for the growth rate of any traits despite the significant GxE in absolute size. Significant genotype-by-time and site-by-time interactions were detected in TLE, SA, and V_{inter} ($P < 0.01$) and TLE, V, and V_{inter} ($P < 0.01$), respectively. A significant fixed effect of genotype was present in TLE, V, and V_{inter} ($P < 0.05$). Growth rate in all traits exhibited a significant fixed effect of time ($P < 0.0001$). Growth rate increased with increasing initial size and time in all traits ($P < 0.0001$, *SI Appendix*, Fig. S7), but standardized growth, calculated as growth rate per unit of existing tissue following (59), decreased with size (*SI Appendix*, Fig. S8). Fixed effects of outplant site were only evident in V ($P = 0.03$), while variation among arrays within sites was nonsignificant in V and SA despite significant array effects on TLE and V_{inter} ($P < 0.05$).

The Capacity for Morphological Plasticity is Correlated with Improved Survival and Growth. Genotype-by-site interactions in the absolute size and shape of colonies indicate significant variation in the capacity for morphological plasticity among genets. We quantified this plasticity using a joint regression analysis (60), which integrates trait data across multiple sites to provide a genotype-specific value of plasticity relative to the population. Plasticity scores ranged from −0.27 to 2.87 and from −0.57 to 5.42 for size- and shape-related traits, respectively (*SI Appendix*, Tables S12 and S13). Plasticity scores above 1 were almost always associated with negative intercept values, while scores below 1 had a large range of positive and negative intercepts. While G1 and G50 were consistently the most plastic genets across time for size-related traits, the most plastic genet in shape-related traits was variable across traits and time points (*SI Appendix*, Tables S12 and S13). We found consistent correlations between the degree of size-related trait plasticity, overall mortality risk, and mean growth rate that support an adaptive role (Fig. 4*A*). Negative relationships between plasticity in absolute size in TLE, SA, V, V_{inter}, and risk score, indicating reduced mortality in more plastic genotypes, strengthened over time (*SI Appendix*, Fig. S9). Similarly, relationships between average growth rate in TLE and trait plasticity began as neutral/weakly positive and progressed to strong positive correlations over time, with the strongest correlations found after 12 mo (*SI Appendix*, Fig. S10). Growth rate tended to be negatively correlated with mortality risk, although significant relationships were only observed at later time points (*SI Appendix*, Fig. S11).

For shape-related traits, no relationship between plasticity and risk score was detected for SA-to-TLE ratio, sphericity, or convexity (*SI Appendix*, Fig. S12). However, SA-to-V ratio showed a significant negative correlation between trait plasticity and risk score at T9 ($R = -0.64$, $P = 0.047$) but no significant relationships at any other time point ($R = -0.2$ to -0.054, $P = 0.58$–0.88). Similarly, plasticity in packing was negatively correlated with risk score only at T12 ($R = -0.74$, $P = 0.014$). Plasticity in shape-related traits was rarely correlated with growth rate in TLE apart from a single positive relationship between plasticity in sphericity and growth rate at T9 ($R = 0.7$, $P = 0.025$, *SI Appendix*, Fig. S13).

Ramets surviving to T12 with no fragmentation represent colonies occupying a morphospace in which survival and growth are uninterrupted by fragmentation. Therefore, we used this subset of ramets to determine if and how the final morphologies differed between sites and genets. When plotted in multivariate trait space, ramets did not cluster by genet or site (Fig. 4*B* and *SI Appendix*, Fig. S14). However, ramets of genets showing higher average survival occupy a broader area, or trait space, compared to genets with lower survival (Fig. 4*B*).

Variation among Offshore Reefs May Contribute to Site-Specific Growth and Survival. Benthic temperatures were recorded hourly at all sites for the one-year experimental period except for Looe Key where data from April 2018 to October 2018 were missing due to a flooded logger (*SI Appendix*, Fig. S15). Therefore, the temperature profiles of eight sites were used to analyze thermal differences among reefs. Water temperatures over the experimental period

Downloaded from https://www.pnas.org by NOAA CENTRAL LIBRARY on January 11, 2024 from IP address 137.75.80.24.

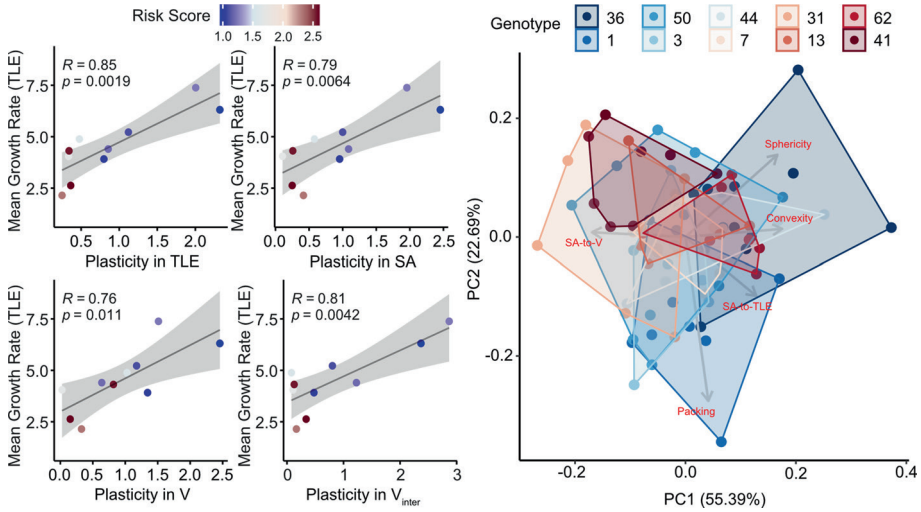

Fig. 4. Morphological plasticity and its relationship to growth and survival. (*A*) Relationship between genet plasticity in final (T12) absolute size and average genet growth rate in TLE over the final 3 mo of the outplant period. Points are colored by genet mortality risk score. Line and shaded region shows line of best fit and 95% confidence interval for each relationship, respectively. (*B*) Principal component analysis of size-independent morphological traits: sphericity, convexity, packing (58), and SA-to-V ratio and SA-to-TLE ratio (gray vectors labeled in red). Points represent individual ramets colored by genet identity (n = 5–12 ramets per genet) by decreasing survival from blue to red. Shaded regions (colored by survival rank) frame the most extraneous ramets for each genet and outline the morphospace occupied by a genet.

were similar between sites (Fig. 1*D* and *SI Appendix*, Table S14). Annual mean temperatures varied by 0.213°C between the warmest (EDR) and coolest (Bahia Honda) sites. Annual temperature ranges varied from 10.12°C (E. Sambo) to 12.26°C (Bahia Honda), while average daily temperature ranges varied from 0.59°C (Marker 32) to 0.71°C (Bahia Honda). Big Pine experienced the most days where the temperature was at or above 30.5°C (69 d), while Bahia Honda experienced the fewest (54 d). Interestingly, Big Pine and Bahia Honda both had the most days above 32°C (3 d), while the majority of sites never reached this temperature throughout the entire experimental period. Summer thermal predictability, calculated as the sum of positive temporal autocorrelation from July through September, was highest at W. Sambo and lowest at Bahia Honda. The three sites with the highest survival probability had the three highest thermal predictability values.

Site-specific biogeochemical parameters, obtained from the long-term Southeast Environmental Research Center (SERC) water quality monitoring program (56), did not significantly differ between sites when restricting the dataset to the experimental period. However, analysis of the full historical dataset (1995–2019) revealed significant differences in nitrate and silica dioxide concentrations among the nine reef sites ($P < 0.05$, *SI Appendix*, Table S15). A principal component analysis of all thermal and water quality parameters showed large aggregate differences between sites despite this limited variation in individual parameters (Fig. 1*E* and *SI Appendix*, Figs. S16 and S17). Sites with the highest survival (E. Sambo, Marker 32, and W. Sambo) clustered together, while the remaining sites were broadly distributed. These high survival sites were also associated with high thermal predictability and historical high average light attenuation (*SI Appendix*, Fig. S17). Bahia Honda, the site with the lowest survival and growth, consistently stood out as the most extreme point (Fig. 1*E* and *SI Appendix*, Figs. S16 and S17).

After removing highly correlated water quality metrics, eleven parameters were used as candidate variables in a Bayesian negative binomial generalized linear model to assess their power to predict changes in coral morphology and mortality risk. Average temperature was significantly negatively associated with the change in TLE, SA, V, and V_{inter} (Fig. 1*F*, *SI Appendix*, Figs. S18–S21), while average daily temperature range was negatively associated with only V_{inter}. Days above 30°C were significantly positively associated with change in V_{inter}, but no patterns were evident for other traits (*SI Appendix*, Figs. S18–S21). Risk score was not significantly associated with any of the environmental parameters (*SI Appendix*, Fig. S22).

Discussion

The presence of a significant GxE interaction indicates that individuals differ in their sensitivity to environmental variation. This variation in reaction norm slope among individuals can reduce prediction accuracy and confound selective breeding programs (61). Here, we identify significant GxE in the size, shape, and ultimate survival of restoration lines of *A. cervicornis,* indicating that no single genet "wins" in all contexts when considering the change in mean trait values across environments. However, the existence of GxE also means that there is genetic variation in the capacity for plasticity, or the degree of environmental responsiveness of individual genotypes. Rather than mean size, we find that this plasticity, or the degree to which a genet is able to change its size relative to the population mean across sites, is positively correlated with overall growth rate and survival. This suggests that plasticity may continue to evolve, although context-dependent trade-offs and the capacity to predict environmental variation, as well as the degree to which plasticity is attributable to host genetics, or specific host–endosymbiont combinations, will likely influence the ultimate trajectory. Below we consider potential drivers and implications of this adaptive plasticity for ecoevolutionary dynamics as well as its applied relevance for the conservation and restoration of reefs.

Adaptive Phenotypic Plasticity in Coral. Phenotypic plasticity can facilitate acclimatization over space and time by allowing organisms to match local trait optima (6, 62). In reef-building corals, plastic responses in morphology (44, 63), bleaching (43), gene expression (52), and gene body methylation (64) alter colony phenotype in ways that are hypothesized to be beneficial, especially in the context of a stress response. In the

Downloaded from https://www.pnas.org by NOAA CENTRAL LIBRARY on January 11, 2024 from IP address 137.75.80.24.

absence of other performance data, however, it was unclear whether such individual plasticity would result in a net fitness benefit, particularly if significant costs were incurred by plastic individuals in nonstress contexts. Here, by explicitly linking morphological plasticity with global growth and survival across sites, rather than a single condition, we show that an individual's ability to be plastic yields a net positive fitness outcome as *A. cervicornis* are exposed to changing environmental conditions. Specifically, increased plasticity, particularly in size-related traits, was associated with a higher average growth rate and increased probability for survival (decreased mortality risk, Fig. 4*A*), strongly supporting an adaptive role.

Coral morphology is an important environmental interface as changes in size and shape can adjust the flow, temperature, and pH in and around a colony (65,66), affecting both normal processes, such as nutrient uptake, and responses to thermal or acidification stress (67–69). In the Florida Keys, spatially or temporally variable conditions, such as temperature, can select for local phenotypic optima (70, 71), and these shifting optima may ultimately be promoting the overall persistence of plastic *A. cervicornis* genotypes. Although sites did not appear to select for specific morphologies in terms of their clustering patterns, genets with the highest average survival occupied a broader morphospace (Fig. 4*B*), again supporting an adaptive role for morphological plasticity.

Coral meet many of the conditions predicted to favor the evolution of increased plasticity (14). Long generation times, high habitat heterogeneity across dispersal ranges, high potential for (assisted) migration, and climate change all expand the range of environments *A. cervicornis* individuals experience within their lifetime (72, 73). Assuming a host genetic basis to plasticity, positive selection in the form of increased survival and/or reproduction of more plastic individuals can enable genetic accommodation, making future generations more plastic (6). This evolution of plasticity may be modulated by strong selection events occurring in *A. cervicornis* and other reef-building coral in the form of disease or bleaching events (40, 74), although the magnitude and direction of the effects will depend on the relationship between morphological plasticity and the response to stress.

However, the evolutionary trajectory may be more complex if plasticity is a product of both host and endosymbiont genotype (GxGxE). The type of dinoflagellate endosymbiont hosted by a coral can alter nutrient exchange, holobiont growth, and thermal tolerance, among other traits (75–77), suggesting that the identity of the endosymbiont could influence the host's ability to express morphological plasticity. If there is a heritable component to host–symbiont specificity (e.g., ref. 78) and preferred strains are readily available, then plasticity may evolve more rapidly. Otherwise, the environmental availability of favored endosymbionts may limit both the expression of morphological plasticity and its evolution. Although genets in this experiment were dominated by *Symbiodinium fitti* as expected (79, 80), strain-level variation was also detected (*SI Appendix*, Fig. S23 and Tables S16 and S17). Shared variation among genets was limited, but when observed was not associated with the capacity for plasticity. For example, some of the most plastic (G1) and least plastic (G62) genets hosted the same symbiont strain (*SI Appendix*, Table S16), suggesting that plasticity is not the result of symbiont identity alone. Additional work is needed to evaluate the fidelity of strain-specific associations in *A. cervicornis* genets over time and environmental availability of strains, in addition to manipulative experiments to specifically quantify GxGxE in this system.

While we did not detect any trade-offs between plasticity and overall growth rate and survival in ambient conditions, the most plastic genets were not always the largest colonies at every site (e.g., *SI Appendix*, Figs. S4-S6), suggesting potential site-specific trade-offs between these traits. Exploring additional costs or limits to morphological plasticity using larger within-site replication will be an important next step in understanding the future adaptive potential of plasticity, particularly in the face of new environmental extremes. Warming ocean temperatures are an ever-present threat to coral reefs, and trade-offs between plasticity and bleaching tolerance or recovery would severely limit the benefits of morphological plasticity as bleaching events become more frequent and severe (39, 40).

Genotype–Environment Interactions Limit Survival and Growth Predictions. Survival and growth rate are two metrics commonly used to evaluate coral fitness because improved survival will positively impact population demographic rates (81–83) while faster growth can shorten the time to reproductive maturity (84). Although lifetime reproductive success is difficult to measure in annual broadcast spawning species such as coral, greater reproductive capacity has been observed in larger colonies (84). Significant variation in the Cox Proportional Hazard risk scores indicated that some genotypes (G41, G62, G13) were at greater risk of mortality than others. Similarly, reef sites also varied in their ability to support coral survival. These results align with previous findings of strong genotype and site effects on coral survival (32, 33) and suggest that certain genets (G36) and reef sites (E. Sambo) may be of higher quality overall. When looking at the remaining genets and sites, however, genotype-by-site interactions for survival and lack of preservation in the rank order of genet survivorship between reef sites (Fig. 2*C*) indicate a limited ability to predict outcomes based on knowledge of genotypes or sites in isolation. This stands in contrast to a similar in situ transplant experiment by Drury et al. (33) that found site effects but no effect of genotype or the interaction on mortality. However, corals in this prior study endured a thermal bleaching event, and variation in mortality was attributed to variation in bleaching among reef sites (33). While no bleaching was observed during the course of this experiment, our results indicate that under normal conditions, genet survivorship from a single site alone does not predict survival in other, even geographically neighboring, reefs.

Similarly, coral morphology appears to be influenced by a complex set of interacting factors that ultimately preclude identification of a globally top-performing individual or "super coral" (34). Genotype-by-site interactions were evident in absolute size and shape, which resulted in a different collection of genets representing the largest relative coral at each site after the 12-mo outplant period (Fig. 3). This evidence of GxE in *A. cervicornis* morphology builds on earlier work in other branching coral species (53, 54, 85). It is important to note that statistical models included corals that experienced fragmentation, as this is an ecologically relevant phenomenon contributing to clonal reproduction (86) and also showed significant effects of site and genotype, the latter of which suggests that aspects of coral growth can also influence their propensity for fragmentation. When we excluded fragmentation, significant genotype-by-site interactions disappeared. Similarly, Drury et al. (33) excluded negative growth and showed independent impacts of genotype and environment on TLE in *A. cervicornis*, but no GxE was detected. While significant fixed effects of genotype on growth rate for TLE, SA, V, and V_{inter} suggest that the intrinsic growth rate varies among genets, GxE in final size is driven by growth and fragmentation, the latter of which can be influenced by colony shape (87), skeletal density (88), and hydrodynamic characteristics of a reef (89). Ultimately, population demographic and restoration success are based on the size of coral colonies rather than their growth rate, indicating that GxE must

Downloaded from https://www.pnas.org by NOAA CENTRAL LIBRARY on January 11, 2024 from IP address 137.75.80.24.

be accounted for when developing conservation and restoration strategies.

Unlike earlier studies in both *A. cervicornis* (33) and its sister species, *A. palmata* (90), we find no effect of site on the majority of morphological and growth traits despite strong site effects on survival. Once thought of as noise, GxE allows for the presence of phenotypic variation among individuals in the absence of overall site effects and may provide a proximate explanation for their absence here. Alternatively, differences in experimental design may also play a role. Kuffner et al. (90) compared ramets outplanted over a large spatial scale (>300 km) compared to the ~60 km span covered in the present study. Similarly, Drury et al. (33) selected reef sites spanning inshore and offshore zones. Although reefs within the offshore zone vary in environmental conditions(56), larger differences are evident between inshore and offshore reefs in temperature, turbidity, and nutrients (56, 91), which may have driven the pronounced site effects on morphology reported earlier (33). Temporal variability in environmental stress can create periods of poor growth or high fragmentation followed by periods of recovery that may mask mean site effects and instead generate a site-by-time signal. We did observe significant site-by-time effects on the majority of morphological traits, indicating that site effects are likely to be time dependent. Finally, significant random effects of array nested within site were present for nearly all morphology traits evaluated and while array effects were not incorporated into Cox Proportional Hazard models due to low replication, anecdotally, arrays at certain sites showed high variability in survival. This suggests that microhabitat variation also contributed to coral size and shape, but investigations into the causes of these patterns will require higher spatial resolution and replication than what was used here.

The Importance of Fragmentation. Fragmentation is a vital part of the evolutionary ecology of *A. cervicornis* as it can significantly alter the demographic trajectory of populations through asexual propagation (86, 89), partial mortality, or death (87). In this experiment, instances of fragmentation had obvious negative impacts on colony size but were mostly nonfatal. This suggests that fragmentation can also impact growth beyond the immediate response to injury, such as increased productivity due to size-dependent growth rates that occur after size reduction (59). While sometimes considered random, fragmentation in this study occurred significantly more in some genets and sites. Differences in calcification rate among *A. cervicornis* genets (88, 92) mean that certain individuals can produce more dense skeletons faster, potentially making them less prone to fragmentation. Moreover, calcification is energetically expensive (93), and apparent tradeoffs in skeletal density and colony size (88, 92) suggest different strategies for skeletal growth in this species that may lead to variation in the ability to withstand physical stress leading to fragmentation.

Spatial and temporal variation in hydrodynamic energy (94, 95), likely, also imposes variable mechanical stress on coral colonies. Coral morphology may respond to these conditions (44, 96), but sudden or especially strong hydrodynamic forces are common sources of damage for branching corals in the Caribbean (97, 98). Human activity may also have contributed to fragmentation and anecdotally, higher tourist activity was observed at Looe Key and EDR. Although fragmentation was usually nonfatal in the focal ramet, we did not track the fate of newly generated fragments precluding determination of the ultimate effect on fitness. Regardless, the existence of nonrandom fragmentation and its influence on ramet performance and GxE reinforce the notion that accounting for fragmentation, rather than treating it as experimental error, will be important for accurately predicting changes in branching coral morphology and performance.

Multivariate Environmental Conditions Distinguish Reefs. The offshore reef sites used here are in an area that has historically been treated as a single environmental unit (56). However, site-specific variation in coral performance (Figs. 2*B* and 3) and in environmental condition (Fig. 1*E*) supports the need for a more nuanced approach. Aggregate differences in abiotic conditions among sites with high average survival appear to be defined by high nitrogen concentrations, thermal predictability, light attenuation/turbidity, and low annual and average daily temperature ranges (*SI Appendix*, Figs. S16 and S17). Similarly, the site with the lowest average survival, Bahia Honda, was differentiated by historically high ranges of nitrite and total phosphorus concentrations, turbidity, and light attenuation (*SI Appendix*, Fig. S17). This site also had the highest annual and daily temperature ranges, but lowest summer thermal predictability during the experimental period. Although no physical or chemical condition was individually correlated with mortality in the Bayesian models, fluctuating environmental conditions have been implicated in the conditioning of marine species to climate change (99, 100). While temperature variability can enhance coral tolerance (101, 102), the predictability of those fluctuations should also impact the ability to acclimate and adapt (103, 104). Thermal predictability was highest among the three sites with the highest survival (E. Sambo, Marker 32, and W. Sambo) and lowest at Bahia Honda, yet no correlations were detected, suggesting the importance of a multivariate approach. The low temporal resolution of water quality metrics precluded obtaining similar measures of predictability in water chemistry during the experimental period. Future work quantifying environmental predictability in addition to fluctuations may yield additional insight into the conditions that support coral performance and plasticity.

Mean temperature was negatively associated with change in size of all morphological traits (Fig. 1*F* and *SI Appendix*, Fig. S18–S21), suggesting that cooler conditions promoted ramet growth. This is unsurprising considering the well-documented negative impact of high temperatures on coral performance (105) and the fact that mean experimental temperatures were within or above the apparent optimum thermal range (ca 25–29°C) for *A. cervicornis* (106, 107). Interestingly, the number of days above 30.5°C seemed to encourage growth in V_{inter} but no other trait. Morphology has been shown to impact flow around a colony, altering heat flux at the coral surface (65, 67), with branching morphologies more capable of offloading heat compared to mounding coral (108). As *A. cervicornis* ramets become less compact by increasing the volume of their interstitial space (Fig. 1*C*), heat dissipation at the coral surface can also be expected to increase through a reduction in the thermal boundary layer (67, 108). While the offshore reef tract of the Florida Keys is typically considered environmentally contiguous, taken together, these results suggest spatial variation in reef conditions independently and cumulatively shape coral performance.

Conclusions

Current coral restoration strategies rely on transplanting clones across reefs varying in abiotic and biotic conditions (33, 37, 55), suggesting that plasticity will play a role in the success or failure of individual colonies. Adaptive morphological plasticity in *A. cervicornis* may enable genets to maintain fitness in response to changes in environmental conditions over time or space. Continued positive selection on intraspecific variation in plasticity,

Downloaded from https://www.pnas.org by NOAA CENTRAL LIBRARY on January 11, 2024 from IP address 137.75.80.24.

contingent on its freedom from trade-offs, should promote the evolution of plasticity and therefore the acclimatory benefits associated with it. Environmental conditions can also promote or constrain the evolution of phenotypic plasticity (10, 103), and while there appears to be sufficient variation within the *A. cervicornis* habitat range to induce plasticity at present, its relative benefits will likely also be dependent on the ability to predict environmental fluctuations, which may prove challenging in the face of continued climate change.

Materials and Methods

Experimental Design. Ten coral genets, sourced from the lower Florida Keys (*SI Appendix*, Fig. S1) and maintained long term (5+ y) at Mote Marine Laboratory's in situ coral nursery, were outplanted in a multisite transplant study under FKMNS permits 2015-163-A1 and 2018-035. In April 2018, 270 coral (mean TLE of 8.4 cm) ramets representing 10 genets (27 ramets per genet) affixed to concrete pucks were photographed following Million et al. (109) and manually measured for TLE immediately before transplantation to nine active restoration sites (*SI Appendix*, Table S1 and Fig. 1).

Three ramets per genet (n = 270 fragments) were randomly outplanted at each site, with one ramet allocated to each of the three ten coral arrays (Fig. 1*A*). Coral pucks were attached to bare reef substrate using marine epoxy over 4 d, from April 21 to April 25. Outplant sites were resurveyed in July 2018, October 2018, January 2019, and April 2019. Ramets were individually rephotographed and measured by-hand at the first four time points for TLE. Survivorship was recorded during site surveys and later confirmed with photographs. Fragmentation was recorded via the photographic time series and through negative growth measures in the resulting trait dataset (*SI Appendix*, *Supplemental Methods*). Ramets where both the coral tissue and ceramic puck were missing indicated technical failure of the marine epoxy rather than a true biological loss and were excluded from subsequent analyses.

Phenotyping. Photographs taken in situ were used to generate individual 3D models of each coral ramet in Metashape 1.5.4 (Agisoft LLC, St. Petersburg, Russia) using a high-throughput pipeline (109). Specifications for model building and all scripts can be found at https://github.com/wyattmillion/Coral3DPhotogram. 3D models were imported into Meshlab v2020.6 (110) to measure four growth-related traits following protocols described in Million et al. (109) and detailed in the *SI Appendix*, *Supplementary Methods*: TLE, SA, V, and V_{inter}. We also assessed the shape of colonies by calculating SA-to-V and TLE-to-V ratios, packing, convexity, and sphericity (58). A subset of ramets were used to evaluate morphology in ramets unaffected by breakage 1 y postoutplant (Fig. 4*B*). In this subset, genets were more equally represented (n = 5–12 ramets per genets) than sites (n = 2–18 ramets per site). These traits were used in a principal components analysis to determine how ramets clustered in morphospace as a function of genet and site.

A. cervicornis genets from the Mote in-water nursery are typically dominated by a single strain of *Symbiodinium fitti*, although background levels of Breviolum, Cladocopium, and Durusdinium have also been reported (79, 80, 111). The dominance of *Symbiodinium* spp. in all experimental ramets was reconfirmed by mapping tag-based RNAseq libraries generated from ramet tissue samples collected at both T0 and T12 (survivors only) to a combination of the *A. cervicornis* reference genome (112) and representative symbiont genomes for the four dominant Symbiodiniaceae genera which associate with reef-building coral: *Symbiodinium microadriaticum* (formerly clade A, (113), *Breviolum minutum* (formerly clade B, (114)), *Cladocopium* spp. (formerly clade C1, (115)), and *Durusdinium trenchii* (formerly clade D, (116)). The relative proportion of reads exhibiting highly unique matches (mapping quality 40 or better) to each genome was used as a proxy for the relative abundance of symbiont genera hosted by each *A. cervicornis* genet (*SI Appendix*, Figs. S23 and S24) following Manzello et al. (71). Prior microsatellite genotyping by Muller et al. (79) revealed genets 3, 7, 13, 41, and 44 are dominated by *S. fitti* strain F421, while G1 associates with F419, and G50 with F423. We reassessed strain-level diversity among genets by mining preexisting SNP data for each focal genet from the Caribbean acroporid genotyping database. Samples previously genotyped using the Axiom Coral Genotyping Array −550962 were rerun through the Axiom Analysis Suite Best Practices Workflow for the algal probes. Of the 531 algal genotyping probes, 439 passed quality control and were kept for downstream analyses. Multilocus genotypes were assigned in R version 4.2.0 using a previously defined threshold of 0.18% (117). A linear discriminant analysis of the signal intensities of a subset of 37 probes was performed to confirm the genus of the dominant symbiont in these genets. *S. fitti* was again found to be the dominant species, but greater diversity was observed among strains as defined by multilocus genotype assignments (*SI Appendix*, Tables S16 and S17).

Environmental Data. All reef sites are located along the offshore reef tract of the Lower Florida Keys at a depth of 5.6 m to 9.1 m. HOBO Pendant Temperature loggers (Onset Computer Corp.; Bourne, MA), set to record hourly, were attached to the reef substrate directly adjacent to the outplanted corals and exchanged with new loggers on subsequent site visits. Hourly temperature records were used to calculate annual mean, annual range, average daily range, maximum monthly mean, days and hours above 30.5°C or 32°C, and summer thermal predictability. Thermal predictability was quantified for July through September only as highly variable temperatures at or above the bleaching threshold of 30.5°C are expected during this window (118). Predictability was calculated as the sum of autocorrelation over a series of lags until autocorrelation reached zero, i.e., the point at which current temperatures are no longer informative of future conditions (119, 120). Quarterly concentrations of benthic nitrite, nitrate, ammonia, dissolved organic and inorganic nitrogen, soluble reactive phosphorus, total phosphorus, total nitrogen, N:P ratio, silicate, dissolved oxygen, total organic carbon, as well as turbidity and light attenuation for each outplant site were obtained from the SERC water quality dataset (Florida International University) associated with each site (Fig. 1*A*, serc.fiu.edu/wqmnetwork/FKNMS-CD/DataDL.htm).

Statistical Analysis. All statistical analyses were performed in R version 3.6.3 (121) and scripts can be found at https://zenodo.org/badge/latestdoi/465475787. Cox Proportional Hazard models were fitted to outplant survival data using the coxme (122) and survival (123) packages. Inclusion of genotype, site, and fragmentation improved model fit, while initial colony size did not and was not significantly associated with survival. Therefore, only genotype, site, and fragmentation were included in the final model. Consistency in genet rank order across sites was quantified with Spearman's correlations. Cumulative link mixed models assessing the ordinal response of fragmentation were implemented with the package ordinal (124) to test for effects of genotype and outplant site on cumulative fragmentation events summed within a ramet over time. Fisher's exact tests were used to determine the enrichment of fragmentation among *A. cervicornis* size classes.

Effects of genotype, site, time, all associated interactions, and initial size on colony morphology (~size) and growth rate in TLE, SA, V, and V_{inter} were tested with linear mixed effects models implemented with the package lmer (125). Fragmentation and outplant array nested within site were included as random effects. When calculating growth rate, ramets experiencing fragmentation (evidenced by a negative growth rate for a ramet over a 3-mo interval) were removed from the dataset and replaced with NA for the time point in which fragmentation occurred.

The extent of plasticity was quantified across each time interval using the joint regression framework (60, 126, 127). This analysis compares the average trait value for a genet at each site and the population average at a respective site to form a linear regression comparing the change in the genet mean trait value to the change in trait value for the entire population. The slope of this regression describes a genet's plasticity relative to the population's plasticity. If the slope is >1, then a genet is more plastic than the population average, and if <1, then a genet is less plastic. We then correlated this unitless measure of plasticity with Cox mortality risk scores and average genet growth rates using Pearson's correlations.

Regression intercepts for highly plastic genets can be used to determine whether increased plasticity was simply a result of higher site-specific growth or greater phenotypic flexibility. High slope values (>1) with negative intercepts indicate more plastic genets that achieve extreme trait values–higher than the population average when high, and lower than the population average when low (*SI Appendix*, Fig. S25). Put another way, these genets would be among the largest in size at high growth sites, but among the smallest at low growth sites. Whereas positive intercepts coupled with shallow slopes indicate genets expressing less plastic trait values across sites.

SERC water quality parameters (56) and thermal characteristics were used to describe environmental variation among reef sites. We calculated both the

Downloaded from https://www.pnas.org by NOAA CENTRAL LIBRARY on January 11, 2024 from IP address 137.75.80.24.

overall mean and the range of benthic nutrient concentrations, turbidity, and light attenuation over the entire length of the SERC dataset (Spring 1995 to Spring 2019) and over the experimental period (April 2018 to 2019). The historical and contemporary SERC data were used to identify differences between reef sites along with high-resolution temperature data collected during the experimental period. An analysis of variance was used to identify significant differences among sites for independent parameters. A principal component analysis was used to explain variation among sites using all parameters simultaneously.

Bayesian negative binomial generalized linear models implemented in R2jags (128) were used to test for the impact of environmental parameters on the growth and survival of ramets at reef sites. Model power was improved by using size, risk score, and environmental data over each of the four time intervals to increase sample size and by removing highly correlated environmental variables.

Data, Materials, and Software Availability. The trait data and scripts used in this study can be found at https://zenodo.org/badge/latestdoi/465475787. Gene expression data used to evaluate symbiont relative abundance can be found at https://www.ncbi.nlm.nih.gov/bioproject/PRJNA594042, while SNP data used to determine strain-level diversity were made publicly available at the Galaxy CoralSNP database (117). [Raw phenotypic and environmental data] data have been deposited in https://zenodo.org/badge/latestdoi/465475787.

ACKNOWLEDGMENTS. We are grateful to Yingqi Zhang, Hunter Ramo, Cory Walter, and Joseph Kuehl for their help in photographing coral in situ. Eric Million helped in design and built equipment for in situ 3D photogrammetry. Phoebe Chang contributed to image preprocessing, and Alexandra Stella and Aryana Volk helped with model validation. Elaina Graham generously facilitated access to the Heidelberg Lab high-performance computer. Training in Bayesian analyses from Dr. Robert van Woesik was facilitated by the NSF Coral Bleaching RCN Early Career Training Program. Fig. 1 was created with BioRender.com. All fieldwork was conducted under permits FKNMS-2015-163-A1 and FKNMS-2018-035. This research was supported by the National Oceanic and Atmospheric Administration Coral Reef Conservation Program grant NA17NOS4820084 and private funding from the Alfred P. Sloan and Rose Hills Foundations.

Author affiliations: [a]Department of Biological Sciences, University of Southern California, Los Angeles, CA 90089; [b]Elizabeth Moore International Center for Coral Reef Research & Restoration, Mote Marine Laboratory, Summerland Key, FL 33042; [c]Department of Biology, The Pennsylvania State University, University Park, PA 16801; and [d]Department of Marine Science, Eckerd College, St. Petersburg, FL 33711

1. S. Des Roches, L. H. Pendleton, B. Shapiro, E. P. Palkovacs, Conserving intraspecific variation for nature's contributions to people. *Nat. Ecol. Evol.* **5**, 574–582 (2021).
2. M. J. West-Eberhard, *Developmental Plasticity and Evolution* (Oxford University Press, 2003).
3. G. G. Simpson, The Baldwin effect. *Evolution* **7**, 110–117 (1953).
4. M. J. West-Eberhard, Phenotypic plasticity and the origins of diversity. *Annu. Rev. Ecol. Syst.* **20**, 249–278 (1989).
5. J. B. Losos *et al.*, Evolutionary implications of phenotypic plasticity in the hindlimb of the lizard Anolis sagrei. *Evolution* **54**, 301–305 (2000).
6. M. Kelly, Adaptation to climate change through genetic accommodation and assimilation of plastic phenotypes. *Philos. Trans. R. Soc. B Biol. Sci.* **374**, 20180176 (2019).
7. C. K. Ghalambor, J. K. McKAY, S. P. Carroll, D. N. Reznick, Adaptive versus non-adaptive phenotypic plasticity and the potential for contemporary adaptation in new environments. *Funct. Ecol.* **21**, 394–407 (2007).
8. A. P. Moczek *et al.*, The role of developmental plasticity in evolutionary innovation. *Proc. Biol. Sci.* **278**, 2705–2713 (2011).
9. Y. Suzuki, H. F. Nijhout, Evolution of a polyphenism by genetic accommodation. *Science* **311**, 650–652 (2006).
10. S. Gavrilets, S. M. Scheiner, The genetics of phenotypic plasticity. V. Evolution of reaction norm shape. *J. Evol. Biol.* **6**, 31–48 (1993).
11. S. M. Scheiner, Genetics and evolution of phenotypic plasticity. *Annu. Rev. Ecol. Syst.* **24**, 35–68 (1993), 10.1146/annurev.es.24.110193.000343.
12. M. Pigliucci, Evolution of phenotypic plasticity: Where are we going now? *Trends Ecol. Evol.* **20**, 481–486 (2005).
13. T. J. Dewitt, A. Sih, D. S. Wilson, Costs and limits of phenotypic plasticity. *Trends Ecol. Evol.* **13**, 77–81 (1998).
14. A. P. Hendry, Key questions on the role of phenotypic plasticity in eco-evolutionary dynamics. *J. Hered.* **107**, 25–41 (2016).
15. J. Van Buskirk, U. K. Steiner, The fitness costs of developmental canalization and plasticity. *J. Evol. Biol.* **22**, 852–860 (2009).
16. J. P. Velotta, Z. A. Cheviron, Remodeling ancestral phenotypic plasticity in local adaptation: A new framework to explore the role of genetic compensation in the evolution of homeostasis. *Integr. Comp. Biol.* **58**, 1098–1110 (2018).
17. M. L. Reaka-Kudla, D. E. Wilson, E. O. Wilson, *Biodiversity II: Understanding and Protecting Our Biological Resources* (Joseph Henry Press, 1996).
18. N. Knowlton *et al.*, "Coral reef biodiversity" in *Life in the World's Oceans: Diversity, Distribution, Abundance*, A. McIntyre, Ed. (John Wiley & Sons, 2010).
19. N. A. J. Graham, K. L. Nash, The importance of structural complexity in coral reef ecosystems. *Coral Reefs* **32**, 315–326 (2013).
20. S. G. Monismith, Hydrodynamics of coral reefs. *Annu. Rev. Fluid Mech.* **39**, 37–55 (2007).
21. A. Lugo-Fernández, H. H. Roberts, W. J. Wiseman Jr., Tide effects on wave attenuation and wave set-up on a caribbean coral reef. *Estuar. Coast. Shelf Sci.* **47**, 385–393 (1998).
22. D. J. Coker, S. K. Wilson, M. S. Pratchett, Importance of live coral habitat for reef fishes. *Rev. Fish Biol. Fish.* **24**, 89–126 (2014).
23. A. M. Szmant, "Nutrient effects on coral reefs: A hypothesis on the importance of topographic and trophic complexity to reef nutrient dynamics" in *Proceedings of the 8th International Coral Reef Symposium*, H. A. Lessios, I. G. Macintyre, Eds. (Smithsonian Tropical Research Institute, Panama, 1997), pp. 1527–1532.
24. H. Cesar, L. Burke, A. L. Pet-Soede, *The Economics of Worldwide Coral Reef Degradation* (International Coral Reef Action Network, 2003).
25. M. S. Pratchett, A. S. Hoey, S. K. Wilson, Reef degradation and the loss of critical ecosystem goods and services provided by coral reef fishes. *Curr. Opin. Environ. Sustainability* **7**, 37–43 (2014).
26. J. W. Porter, O. W. Meier, Quantification of loss and change in floridian reef coral populations. *Integr. Comp. Biol.* **32**, 625–640 (1992).
27. K. L. Cramer *et al.*, Widespread loss of Caribbean acroporid corals was underway before coral bleaching and disease outbreaks. *Sci. Adv.* **6**, eaax9395 (2020).
28. G. Roff, J. Joseph, P. J. Mumby, Multi-decadal changes in structural complexity following mass coral mortality on a Caribbean reef. *Biogeosciences* **17**, 5909–5918 (2020).
29. L. Alvarez-Filip, I. M. Côté, J. A. Gill, A. R. Watkinson, N. K. Dulvy, Region-wide temporal and spatial variation in Caribbean reef architecture: Is coral cover the whole story? *Glob. Chang. Biol.* **17**, 2470–2477 (2011).
30. P. J. Edmunds, Evidence that reef-wide patterns of coral bleaching may be the result of the distribution of bleaching-susceptible clones. *Mar. Biol.* **121**, 137–142 (1994).
31. R. Cunning *et al.*, Census of heat tolerance among Florida's threatened staghorn corals finds resilient individuals throughout existing nursery populations. *Proc. R. Soc. B. Biol. Sci.* **288**, 20211613 (2021).
32. R. Woesik *et al.*, Differential survival of nursery-reared acropora cervicornis outplants along the Florida reef tract. *Restor. Ecol.* **29**, e13302 (2021).
33. C. Drury, D. Manzello, D. Lirman, Genotype and local environment dynamically influence growth, disturbance response and survivorship in the threatened coral, acropora cervicornis. *PLoS One* **12**, e0174000 (2017).
34. E. F. Camp, V. Schoepf, D. J. Suggett, How can "Super Corals" facilitate global coral reef survival under rapid environmental and climatic change? *Glob. Chang. Biol.* **24**, 2755–2757 (2018).
35. S. R. Palumbi, D. J. Barshis, N. Traylor-Knowles, R. A. Bay, Mechanisms of reef coral resistance to future climate change. *Science* **344**, 895–898 (2014).
36. M. O. Hoogenboom *et al.*, Environmental drivers of variation in bleaching severity of acropora species during an extreme thermal anomaly. *Front. Marine Sci.* **4**, 376 (2017).
37. C. N. Young, S. A. Schopmeyer, D. Lirman, A review of reef restoration and coral propagation using the threatened genus acropora in the Caribbean and Western Atlantic. *Bull. Mar. Sci.* **88**, 1075–1098 (2012).
38. O. Hoegh-Guldberg *et al.*, Assisted colonization and rapid climate change. *Science* **321**, 345–346 (2008).
39. O. Hoegh-Guldberg *et al.*, Coral reefs under rapid climate change and ocean acidification. *Science* **318**, 1737–1742 (2007).
40. D. P. Manzello, Rapid recent warming of coral reefs in the florida keys. *Sci. Rep.* **5**, 16762 (2015).
41. K. L. Barott *et al.*, Coral bleaching response is unaltered following acclimatization to reefs with distinct environmental conditions. *Proc. Natl. Acad. Sci. U.S.A.* **118**, e2025435118 (2021).
42. M. K. Morikawa, S. R. Palumbi, Using naturally occurring climate resilient corals to construct bleaching-resistant nurseries. *Proc. Natl. Acad. Sci.* **116**, 10586–10591 (2019).
43. C. Drury, D. Lirman, Genotype by environment interactions in coral bleaching. *Proc. Biol. Sci.* **288**, 20210177 (2021).
44. P. A. Todd, Morphological plasticity in scleractinian corals. *Biol. Rev. Camb. Philos. Soc.* **83**, 315–337 (2008).
45. E. Tambutté *et al.*, Morphological plasticity of the coral skeleton under CO2-driven seawater acidification. *Nat. Commun.* **6**, 7368 (2015).
46. E. M. Muller *et al.*, Heritable variation and lack of tradeoffs suggest adaptive capacity in Acropora cervicornis despite negative synergism under climate change scenarios. *Proc. Biol. Sci.* **288**, 20210923 (2021).
47. M. Ziegler, C. M. Roder, C. Büchel, C. R. Voolstra, Limits to physiological plasticity of the coral Pocillopora verrucosa from the central Red Sea. *Coral Reefs* **33**, 1115–1129 (2014).
48. R. A. Bay, S. R. Palumbi, Rapid acclimation ability mediated by transcriptome changes in reef-building corals. *Genome Biol. Evol.* **7**, 1602–1612 (2015).
49. M. M. Rocker, C. D. Kenkel, D. S. Francis, B. L. Willis, L. K. Bay, Plasticity in gene expression and fatty acid profiles of Acropora tenuis reciprocally transplanted between two water quality regimes in the central Great Barrier Reef, Australia. *J. Exp. Mar. Bio. Ecol.* **511**, 40–53 (2019).
50. M. O. Hoogenboom, S. R. Connolly, K. R. N. Anthony, Interactions between morphological and physiological plasticity optimize energy acquisition in corals. *Ecology* **89**, 1144–1154 (2008).
51. A. G. Grottoli, L. J. Rodrigues, J. E. Palardy, Heterotrophic plasticity and resilience in bleached corals. *Nature* **440**, 1186–1189 (2006).
52. C. D. Kenkel, M. V. Matz, Gene expression plasticity as a mechanism of coral adaptation to a variable environment. *Nat. Ecol. Evol.* **1**, 14 (2016).

Downloaded from https://www.pnas.org by NOAA CENTRAL LIBRARY on January 11, 2024 from IP address 137.75.80.24.

53. J. F. Bruno, P. J. Edmunds, Clonal variation for phenotypic plasticity in the coralmadracis Mirabilis. *Ecology* **78**, 2177–2190 (1997).
54. P. A. Todd, R. J. Ladle, N. J. I. Lewin-Koh, L. M. Chou, Genotype × environment interactions in transplanted clones of the massive corals Favia speciosa and Diploastrea heliopora. *Mar. Ecol. Prog. Ser.* **271**, 167–182 (2004).
55. K. E. Lohr, S. Bejarano, D. Lirman, S. Schopmeyer, C. Manfrino, Optimizing the productivity of a coral nursery focused on staghorn coral Acropora cervicornis. *Endanger. Species Res.* **27**, 243–250 (2015).
56. H. O. Briceño, J. N. Boyer, "2018 Annual report of the water quality monitoring project for the water quality protection program of the florida keys National Marine Sanctuary" (SERC Research Reports. 117, FIU Digital Commons, Miami, Florida, USA 2019) (January 26, 2022).
57. M. S. Pratchett, K. D. Anderson, "Spatial, temporal and taxonomic variation in coral growth–implications for the structure and function of coral reef ecosystems" in *Oceanography and Marine Biology* (CRC Press, Oceanography and Marine Biology: An Annual Review, 2015), pp. 224–305.
58. K. J. A. Zawada, M. Dornelas, J. S. Madin, Quantifying coral morphology. *Coral Reefs* **38**, 1281–1292 (2019).
59. D. Lirman *et al.*, Growth dynamics of the threatened Caribbean staghorn coral acropora cervicornis: Influence of host genotype, symbiont identity, colony size, and environmental setting. *PLoS One* **9**, e107253 (2014).
60. J. R. Stinchcombe, L. A. Dorn, J. Schmitt, Flowering time plasticity in Arabidopsis thaliana: A reanalysis of Westerman & Lawrence (1970). *J. Evol. Biol.* **17**, 197–207 (2004).
61. D. Ly *et al.*, Relatedness and genotype × environment interaction affect prediction accuracies in genomic selection: A study in cassava. *Crop Sci.* **53**, 1312–1325 (2013).
62. S. Via *et al.*, Adaptive phenotypic plasticity: Consensus and controversy. *Trends Ecol. Evol.* **10**, 212–217 (1995).
63. S. Muko, K. Kawasaki, K. Sakai, F. Takasu, N. Shigesada, Morphological plasticity in the coral porites sillimaniani and its adaptive significance. *Bull. Mar. Sci.* **66**, 225–239 (2000).
64. G. Dixon, Y. Liao, L. K. Bay, M. V. Matz, Role of gene body methylation in acclimatization and adaptation in a basal metazoan. *Proc. Natl. Acad. Sci. U.S.A.* **115**, 13342–13346 (2018).
65. J. B. Stocking, C. Laforsch, R. Sigl, M. A. Reidenbach, The role of turbulent hydrodynamics and surface morphology on heat and mass transfer in corals. *J. R. Soc. Interface* **15**, 20180448 (2018).
66. N. C. S. Chan, D. Wangpraseurt, M. Kühl, S. R. Connolly, Flow and coral morphology control coral surface pH: Implications for the effects of Ocean acidification. *Front. Marine Sci.* **3**, 10 (2016).
67. I. M. Jimenez, M. Kühl, A. W. D. Larkum, P. J. Ralph, Effects of flow and colony morphology on the thermal boundary layer of corals. *J. R. Soc. Interface* **8**, 1785–1795 (2011).
68. W. C. Dennison, D. J. Barnes, Effect of water motion on coral photosynthesis and calcification. *J. Exp. Mar. Bio. Ecol.* **115**, 67–77 (1988).
69. M. P. Lesser, V. M. Weis, M. R. Patterson, P. L. Jokiel, Effects of morphology and water motion on carbon delivery and productivity in the reef coral, Pocillopora damicornis (Linnaeus): Diffusion barriers, inorganic carbon limitation, and biochemical plasticity. *J. Exp. Mar. Bio. Ecol.* **178**, 153–179 (1994).
70. C. D. Kenkel, A. T. Almanza, M. V. Matz, Fine-scale environmental specialization of reef-building corals might be limiting reef recovery in the Florida Keys. *Ecology* **96**, 3197–3212 (2015).
71. D. P. Manzello *et al.*, Role of host genetics and heat-tolerant algal symbionts in sustaining populations of the endangered coral Orbicella faveolata in the Florida Keys with ocean warming. *Glob. Chang. Biol.* **25**, 1016–1031 (2019).
72. C. Drury, C. B. Paris, V. H. Kourafalou, D. Lirman, Dispersal capacity and genetic relatedness in Acropora cervicornis on the Florida Reef Tract. *Coral Reefs* **37**, 585–596 (2018).
73. E. M. Hemond, S. V. Vollmer, Genetic diversity and connectivity in the threatened staghorn coral (Acropora cervicornis) in Florida. *PLoS One* **5**, e8652 (2010).
74. D. E. Williams, M. W. Miller, Coral disease outbreak: Pattern, prevalence and transmission in Acropora cervicornis. *Mar. Ecol.: Prog. Ser.* **301**, 119–128 (2005).
75. A. Jones, R. Berkelmans, Potential costs of acclimatization to a warmer climate: Growth of a reef coral with heat tolerant vs. sensitive symbiont types. *PLoS One* **5**, e10437 (2010).
76. N. E. Cantin, M. J. H. van Oppen, B. L. Willis, J. C. Mieog, A. P. Negri, Juvenile corals can acquire more carbon from high-performance algal symbionts. *Coral Reefs* **28**, 405 (2009).
77. P. Buerger *et al.*, Heat-evolved microalgal symbionts increase coral bleaching tolerance. *Sci. Adv.* **6**, eaba2498 (2020).
78. K. M. Quigley, B. L. Willis, L. K. Bay, Heritability of the symbiodinium community in vertically- and horizontally-transmitting broadcast spawning corals. *Sci. Rep.* **7**, 8219 (2017).
79. E. M. Muller, E. Bartels, I. B. Baums, Bleaching causes loss of disease resistance within the threatened coral species Acropora cervicornis. *Elife* **7**, e35066 (2018).
80. J. E. Parkinson *et al.*, Extensive transcriptional variation poses a challenge to thermal stress biomarker development for endangered corals. *Mol. Ecol.* **27**, 1103–1119 (2018).
81. R. C. Babcock, Comparative demography of three species of scleractinian corals using age- and size-dependent classifications. *Ecol. Monogr.* **61**, 225–244 (1991).
82. T. P. Hughes, D. Ayre, J. H. Connell, The evolutionary ecology of corals. *Trends Ecol. Evol.* **7**, 292–295 (1992).
83. M. Álvarez-Noriega *et al.*, Fecundity and the demographic strategies of coral morphologies. *Ecology* **97**, 3485–3493 (2016).
84. V. R. Hall, T. P. Hughes, Reproductive strategies of modular organisms: Comparative studies of reef-building corals. *Ecology* **77**, 950–963 (1996).
85. N. E. Doszpot, M. J. McWilliam, M. S. Pratchett, A. S. Hoey, W. F. Figueira, Plasticity in three-dimensional geometry of branching corals along a cross-shelf gradient. *Diversity* **11**, 44 (2019).
86. C. Drury, J. B. Greer, I. Baums, B. Gintert, D. Lirman, Clonal diversity impacts coral cover in Acropora cervicornisthickets: Potential relationships between density, growth, and polymorphisms. *Ecol. Evol.* **9**, 4518–4531 (2019).
87. J. S. Madin, A. H. Baird, M. Dornelas, S. R. Connolly, Mechanical vulnerability explains size-dependent mortality of reef corals. *Ecol. Lett.* **17**, 1008–1015 (2014).
88. I. B. Kuffner *et al.*, Plasticity in skeletal characteristics of nursery-raised staghorn coral, Acropora cervicornis. *Coral Reefs* **36**, 679–684 (2017).
89. V. Tunnicliffe, Breakage and propagation of the stony coral Acropora cervicornis. *Proc. Natl. Acad. Sci. U.S.A.* **78**, 2427–2431 (1981).
90. I. B. Kuffner, A. Stathakopoulos, L. T. Toth, L. A. Bartlett, Reestablishing a stepping-stone population of the threatened elkhorn coral Acropora palmata to aid regional recovery. *Endanger. Species Res.* **43**, 461–473 (2020).
91. D. Lirman, P. Fong, Is proximity to land-based sources of coral stressors an appropriate measure of risk to coral reefs? An example from the Florida Reef Tract. *Mar. Pollut. Bull.* **54**, 779–791 (2007).
92. K. E. Lohr, J. T. Patterson, Intraspecific variation in phenotype among nursery-reared staghorn coral Acropora cervicornis (Lamarck, 1816). *J. Exp. Mar. Bio. Ecol.* **486**, 87–92 (2017).
93. A. L. Cohen, T. A. McConnaughey, Geochemical perspectives on coral mineralization. *Rev. Mineral. Geochem.* **54**, 151–187 (2003).
94. J. J. Leichter, G. B. Deane, M. D. Stokes, Spatial and temporal variability of internal wave forcing on a coral reef. *J. Phys. Oceanogr.* **35**, 1945–1962 (2005).
95. S. Ahn, K. A. Haas, V. S. Neary, Dominant wave energy systems and conditional wave resource characterization for coastal waters of the United States. *Energies* **13**, 3041 (2020).
96. P. L. Jokiel, C. P. Jury, I. B. Kuffner, "Coral calcification and ocean acidification" in *Coral Reefs at the Crossroads*, D. K. Hubbard, *et al.*, Eds. (Springer, Netherlands, 2016), pp. 7–45.
97. J. D. Woodley *et al.*, Hurricane Allen's impact on Jamaican coral reefs. *Science* **214**, 749–755 (1981).
98. R. D. Perkins, P. Enos, Hurricane Betsy in the Florida-Bahama Area: Geologic effects and comparison with Hurricane Donna. *J. Geol.* **76**, 710–717 (1968).
99. K. J. Kroeker *et al.*, Ecological change in dynamic environments: Accounting for temporal environmental variability in studies of ocean change biology. *Glob. Chang. Biol.* **26**, 54–67 (2020).
100. M. Ziegler *et al.*, Integrating environmental variability to broaden the research on coral responses to future ocean conditions. *Glob. Chang. Biol.* **27**, 5532–5546 (2021).
101. A. Safaie *et al.*, High frequency temperature variability reduces the risk of coral bleaching. *Nat. Commun.* **9**, 1671 (2018).
102. T. A. Oliver, S. R. Palumbi, Do fluctuating temperature environments elevate coral thermal tolerance? *Coral Reefs* **30**, 429–440 (2011).
103. M. C. Bitter *et al.*, Fluctuating selection and global change: A synthesis and review on disentangling the roles of climate amplitude, predictability and novelty. *Proc. Biol. Sci.* **288**, 20210727 (2021).
104. T. E. Reed, R. S. Waples, D. E. Schindler, J. J. Hard, M. T. Kinnison, Phenotypic plasticity and population viability: The importance of environmental predictability. *Proc. Biol. Sci.* **277**, 3391–3400 (2010).
105. B. E. Brown, Coral bleaching: Causes and consequences. *Coral Reefs* **16**, S129–S138 (1997).
106. B. T. Paradis, R. P. Henry, N. E. Chadwick, Compound effects of thermal stress and tissue abrasion on photosynthesis and respiration in the reef-building coral Acropora cervicornis (Lamarck, 1816). *J. Exp. Mar. Bio. Ecol.* **521**, 151222 (2019).
107. E. H. Gladfelter, Skeletal development in Acropora cervicornis. *Coral Reefs* **3**, 51–57 (1984).
108. I. M. Jimenez, M. Kühl, A. W. D. Larkum, P. J. Ralph, Heat budget and thermal microenvironment of shallow-water corals: Do massive corals get warmer than branching corals? *Limnol. Oceanogr.* **53**, 1548–1561 (2008).
109. W. C. Million, S. O'Donnell, E. Bartels, C. D. Kenkel, Colony-level 3D photogrammetry reveals that total linear extension and initial growth do not scale with complex morphological growth in the branching coral, Acropora cervicornis. *Front. Marine Sci.* **8**, 384 (2021).
110. P. Cignoni *et al.*, *MeshLab: An Open-Source Mesh Processing Tool* (Visual Computing Lab, ISTI - CNR, Pisa Italy, 2008).
111. I. B. Baums, M. E. Johnson, M. K. Devlin-Durante, M. W. Miller, Host population genetic structure and zooxanthellae diversity of two reef-building coral species along the Florida Reef Tract and wider Caribbean. *Coral Reefs* **29**, 835–842 (2010).
112. S. A. Kitchen *et al.* Genomic Variants Among Threatened Acropora Corals. *G3* **9**, 1633–1646. (2019).
113. M. Aranda *et al.*, Genomes of coral dinoflagellate symbionts highlight evolutionary adaptations conducive to a symbiotic lifestyle. *Sci. Rep.* **6**, 39734 (2016).
114. E. Shoguchi *et al.*, Draft assembly of the Symbiodinium minutum nuclear genome reveals dinoflagellate gene structure. *Curr. Biol.* **23**, 1399–1408 (2013).
115. E. Shoguchi *et al.*, Two divergent Symbiodinium genomes reveal conservation of a gene cluster for sunscreen biosynthesis and recently lost genes. *BMC Genomics* **19**, 458 (2018).
116. K. E. Dougan *et al.*, Whole-genome duplication in an algal symbiont serendipitously confers thermal tolerance to corals. bioXriv [Preprint] (2022). https://doi.org/10.1101/2022.04.10.487810.
117. S. A. Kitchen *et al.*, STAGdb: A 30K SNP genotyping array and science gateway for Acropora corals and their dinoflagellate symbionts. *Sci. Rep.* **10**, 12488 (2020).
118. D. P. Manzello, R. Berkelmans, J. C. Hendee, Coral bleaching indices and thresholds for the Florida Reef Tract, Bahamas, and St. Croix, US Virgin Islands. *Mar. Pollut. Bull.* **54**, 1923–1931 (2007).
119. J. E. Walsh, I. Shapiro, T. L. Shy, On the variability and predictability of daily temperatures in the Arctic. *Atmos.-Ocean* **43**, 213–230 (2005).
120. J. Li, R. Ding, Temporal-spatial distribution of the predictability limit of monthly sea surface temperature in the global oceans. *Int. J. Climatol.* **33**, 1936–1947 (2013).
121. R Core Team, *R: A Language and Environment for Statistical Computing* (R Foundation for Statistical Computing, Vienna, Austria, 2020).
122. T. M. Therneau, *coxme: Mixed Effects Cox Models* (version 2.2-14123, Comprehensive R Archive Network (CRAN), 2020).
123. T. M. Therneau, T. Lumley, E. Atkinso, C. Crowson, *survival: Survival Analysis* (version 3.3-1128, Comprehensive R Archive Network (CRAN), 2022) (March 3, 2022).
124. R. H. B. Christensen, *Regression Models for Ordinal Data* (version 2019.12-10, 2019).
125. D. Bates *et al.*, *Linear Mixed-Effects Models using "Eigen" S4* (version 1.1-29, Journal of Statistical Software, Innsbruck, Austria, 2022).
126. F. Yates, W. G. Cochran, The analysis of groups of experiments. *J. Agric. Sci.* **28**, 556–580 (1938).
127. L. A. Dorn, E. H. Pyle, J. Schmitt, Plasticity to light cues and resources in Arabidopsis thaliana: Testing for adaptive value and costs. *Evolution* **54**, 1982–1994 (2000).
128. Y.-S. Su, M. Yajima, R2jags: Using R to Run "JAGS" (version 0.7-1, Comprehensive R Archive Network (CRAN), 2021) (March 2, 2022).

Downloaded from https://www.pnas.org by NOAA CENTRAL LIBRARY on January 11, 2024 from IP address 137.75.80.24.